

Comparing analysis of heart rate and blood pressure fluctuations in healthy subjects

Katharina Fuchs, Aicko Y. Schumann, Anja Kuhnhold, Przemyslaw Guzik, Jaroslaw Piskorski, Georg Schmidt and Jan W. Kantelhardt

Abstract—Heartbeat interval fluctuations exhibit fractal scaling behavior on certain time scales. However, less is known about blood pressure fluctuations and respiration. We compare the short-term and long-term scaling properties of heartbeat intervals (HBI), systolic (SBP) and diastolic (DBP) blood pressure as well as respiratory (RES) time series based on recordings from 127 healthy subjects using centered moving average (CMA) analysis and detrended fluctuation analysis (DFA1). We find that both methods are equivalent and long-term correlations of all four signals are similar, $\alpha_{2,HBI} = 0.86 \pm 0.15$, $\alpha_{2,SBP} = 0.83 \pm 0.14$, $\alpha_{2,DBP} = 0.75 \pm 0.15$, and $\alpha_{RES} = 0.68 \pm 0.07$. However, short-term exponents are strongly increased for blood pressure, $\alpha_{1,SBP} = 1.26 \pm 0.20$ and $\alpha_{1,DBP} = 1.19 \pm 0.17$ compared with $\alpha_{1,HBI} = 0.87 \pm 0.23$ for heartbeat. These results suggest that the long-term regulation of heart-rate and blood pressure is controlled in a similar fashion. The control of short-term fluctuations, however, is clearly different, with a non-stationary behavior of the blood pressure fluctuations. We also calculate baroreflex sensitivity using the dual sequences method and study the cross-correlations between all exponents and baroreflex sensitivities.

Index Terms—heart rate, blood pressure, respiration, scaling, baroreflex sensitivity, long-term correlations

I. INTRODUCTION

Long-term power-law correlations in electro-physiological signals from the human autonomic system have been studied for many years, e. g., in heartbeat dynamics [1-7], blood pressure [8-9], respiration dynamics [7,10-12], brain waves [13-15], and gait time series [16-17]. Such correlations characterize a persistent variation of the considered signal on many time scales. For example, the probability of persistently larger (or smaller) values over extended periods of time is characteristically increased. Long beat-to-beat intervals are more likely to be followed by long intervals than by short ones, and vice versa.

The correlation structure of the data can be classified by fractal or multifractal scaling analysis [3-5]. Calculated scaling exponents are affected by pathologic conditions, sympathovagal balance, cardiopulmonary regulation, and circadian rhythm, paving the way towards an identification and discrimination of physiologic states, such as exercise versus rest,

wake versus sleep, across circadian phases, or different sleep stages [4,6] and for the development of diagnostic markers for diseases or physiologic risks, such as cardiac risk.

While the scaling behavior of heartbeat fluctuations has been thoroughly studied for many years, there are much fewer studies on respiration [7,10-12] and hardly any study on blood pressure fluctuations in healthy subjects. The reason is the large effort required for continuously recording blood pressure over an extended time period. While Baumert, Baier and Voss studied recordings of 30 minutes duration from 27 healthy controls (besides 25 patients with dilated cardiomyopathy) [8] (see also Voss et al. [18]), Castiglioni et al. have recently analyzed 10 minutes of non-stationary data recordings from 60 healthy subjects [9]. Neither study, however, focused on a direct comparison of heartbeat and blood pressure scaling properties, which could help to elucidate the corresponding regulation mechanisms of the autonomic nervous system.

In this paper we compare the scaling behavior of heartbeat fluctuations with the scaling behavior of blood pressure fluctuations in a large group of 127 healthy young subjects (age 19-30 years). All signals were recorded simultaneously for 30 minutes; the subjects were in supine position under resting conditions. We find that, unlike heartbeat intervals, blood pressure values fluctuate in a non-stationary way on short time scales characterized by effective scaling exponents $\alpha_1 > 1$. On long time scales, on the other hand, the fluctuations of heartbeat intervals and blood pressure values are very similar and both remain in the stationary regime with $\alpha_2 < 1$. Our results suggest that a recent analysis of blood pressure fluctuations in 11 rats [19], where somewhat similar scaling behavior was observed and long-term scaling behavior of blood pressure was shown to be due to baroreflex control, is probably also valid for humans. Therefore, we analyze baroreflex sensitivity, obtaining the surprising result that it is cross-correlated most noticeably with respiration fluctuations – a possible hint towards the gating theory for the relation of respiration and baroreflex [20].

II. DATA AND METHODS

A. Data

The database used for this work contains recordings from 127 healthy subjects with a duration of approximately 30 minutes. ECG, finger arterial blood pressure, and respiratory signals were recorded from spontaneously breathing subjects in supine position. Three-channel chest ECG and respiratory curves (piezoelectric belt placed at the level between xyphoid and umbilicus) were directly recorded at a sampling frequency

K.F., A.K. and J.W.K. are with the Institute of Physics, Martin-Luther-University Halle-Wittenberg, 06099 Halle, Germany, email: jan.kantelhardt@physik.uni-halle.de

A.Y.S. is with the Complexity Science Group at the Department of Physics and Astronomy, University of Calgary, Canada

P.G. is with the Department of Cardiology, University of Medical Sciences, Poznan, Poland

J.P. is with the Physics Department, University of Zielona Gora, Poland

G.S. is with the 1. Medizinische Klinik, Technical University Munich, Germany

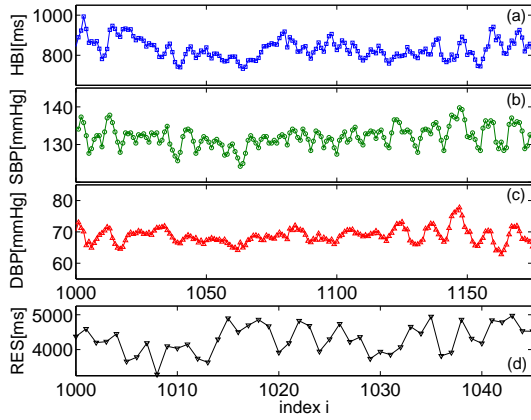


Fig. 1. Four exemplary fragments from (a) HBI, (b) SBP, (c) DBP, and (d) RES time series recorded from a typical young healthy subject.

of 1600 Hz by an A/D converter (Porti 5, TMSI, The Netherlands). The finger blood-pressure signal was recorded non-invasively by Portapres (FMS, The Netherlands) and directly sent to the A/D converter for synchronization with ECG and respiration. From this we determined the series of time intervals between successive heartbeats (heartbeat intervals, HBI), the corresponding systolic blood pressure (SBP) and diastolic blood pressure (DBP) series, as well as the respiratory (RES) time intervals between successive breaths using the software LIBRASCH [21]. Figure 1 shows parts of the data for a typical subject.

B. Centered Moving Average Analysis (CMA)

Like the well-known Detrended Fluctuation Analysis (DFA, see next subsection), the method of Centered Moving Average (CMA) analysis [22] is based on the random walk theory. We refer the reader to [23] for a recent comparison of the methods. CMA allows to determine the correlation properties of a time series $(x_i), i = 1, \dots, N$ (with mean $\langle x \rangle = N^{-1} \sum_{i=1}^N x_i$). Firstly, the 'profile' function

$$X(n) = \sum_{i=1}^n (x_i - \langle x \rangle) \quad (1)$$

is calculated, i. e., the data is integrated. In the second step one calculates a running average by averaging all data points of the profile function within a region of length (scale) s around each point n ,

$$\tilde{X}_s(n) = \frac{1}{s} \sum_{j=-(s-1)/2}^{(s-1)/2} X(n+j). \quad (2)$$

Note that s must be an odd number and that $s < s_{max} \approx N/4$ should not be exceeded due to insufficient statistics for the larger scales. In the third step, the centered moving average from Eq. (2) is used to detrend the profile, eliminating all trends on scales above s . The fluctuation function on scale s is determined by the square root of the variance of $X(n) - \tilde{X}_s(n)$,

$$F(s) = \left[\frac{1}{N} \sum_{n=1}^N (X(n) - \tilde{X}_s(n))^2 \right]^{1/2} \quad (3)$$

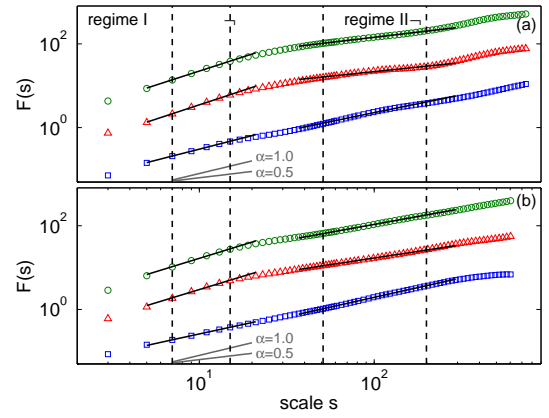


Fig. 2. CMA fluctuation functions for HBI (blue squares), SBP (green circles) and DBP (red triangles) for two representative subjects (a,b). The fitting regimes are marked by vertical dashed lines and fitted slopes are indicated by black continuous lines. Similar plots are obtained for DFA1.

The fluctuation function is assumed to scale as

$$F(s) \propto s^\alpha \quad (4)$$

with an effective scaling exponent α . The value of α can be calculated via a linear fit to the double-logarithmic plot of $F(s)$ versus s , see Fig. 2. If $\alpha = 1/2$, then there are no correlations or only short-term correlations in the data. A value $\alpha > 1/2$ indicates that the data are long-term correlated, so that a large (small) value is followed by another large (small) value on all time scales. If the data is stationary, i. e., $\alpha < 1$, the relation $\gamma = 2 - 2\alpha$ gives the correlation exponent γ characterizing the long-term decay of the autocorrelation function $C(s) = \langle (x_i - \langle x \rangle)(x_{i+s} - \langle x \rangle) \rangle \sim s^{-\gamma}$. For non-stationary data, i. e. $\alpha > 1$, however, the mean $\langle x \rangle$ depends on the length N of the data series. In this case, the root-mean-square displacement $\sqrt{(x_i - \langle x \rangle)^2}$ increases with i , and the values of the time series will diverge asymptotically for N (and i) going to infinity. This cannot happen in medical time series of course, and therefore, regulation mechanisms, restricting the long-term scaling exponent α to values below unity, are needed. We will see in the following that exactly this is achieved by the baroreflex mechanism.

Figure 2 shows $F(s)$ for HBI, SBP, and DBP for two typical subjects. One can see that there is a crossover in the scaling behavior of the blood pressure signals, but hardly any crossover for HBI. To characterize the data of all 127 subjects and to compare the scaling behaviors, we have fitted straight lines to the log-log plots in the two marked regimes, $7 \leq s \leq 15$ for exponent α_1 (short-term regime) and $51 \leq s \leq 199$ for exponent α_2 (long-term regime). For respiratory intervals, the fitting range is $13 \leq s \leq 49$ (long-term regime only; recall that respiration is approx. four times slower than heartbeat). These ranges are in agreement with those commonly used in heartbeat data analysis, see e. g. [7].

C. Detrended Fluctuation Analysis (DFAI)

The DFA [4,24-25] is rather similar to the CMA method described in the previous subsection. The only change is a replacement of the detrending procedure used to calculate

$\tilde{X}_s(n)$, i. e. a different Eq. (2). Here, the profile function is divided into non-overlapping segments of length s , and separate linear fits are performed in each segment to define $\tilde{X}_s(n)$. In this case, $\tilde{X}_s(n)$ is not smooth, since it consists of linear patches with discontinuities at the segment boundaries. Hence, DFA has some minor drawbacks compared with CMA if s is very small or very short time series are considered; see [23] for a thorough discussion. DFA, on the other hand, has the clear advantage that higher order trends in the data can be removed by fitting higher order polynomials instead of straight lines within each segment [4]. In this case, however, DFA becomes computationally more expensive due to the involved fitting procedures. Additionally, this approach leads to a loss of degrees of freedom, which can be severe with short segments and high-order polynomials; this is in fact the reason for the known systematic deviation of DFA curves for small s [25,23]. In this study we use only linear DFA (DFA1) and compare the results with those from CMA.

D. Dual Sequence Method for Baroreflex Sensitivity

The baroreflex is an important feedback mechanism to maintain physiological blood pressure values. Its function is quantified by the baroreflex sensitivity (BRS) index. In this study we determine BRS using a widely approved and applied time-domain based method, the dual sequence method, see e. g. [26]. Within time series of HBI and SBP, sequences with unidirectional behavior (either decreases or increases) of both, SBP and HBI, and a minimum length of three successive values are selected. This is done separately for increases in SBP and HBI (lengthenings, slowing down), and for decreases in SBP and HBI (shortenings, accelerations). For each sequence the slope of the regression line between SBP and HBI is calculated. Then one averages over all slopes and obtains a coefficient of the dimension $\text{ms} \cdot (\text{mmHg})^{-1}$ representing BRS.

III. RESULTS AND DISCUSSION

Table I summarizes the average fluctuation exponents obtained from all 127 subjects for HBI, SBP, and DBP, as well as RES time series, comparing the results of CMA and DFA1. There is very good agreement between the results of both methods. When CMA is used, some values of α are slightly smaller, which, however, is due to a known systematic deviation of DFA curves for small s [25,23].

TABLE I
AVERAGE FLUCTUATION EXPONENTS OBTAINED FOR ALL 127 SUBJECTS FOR HBI, SBP, DBP AND RES TIME SERIES, COMPARING THE RESULTS OF CMA AND DFA1.

	CMA	DFA1
$\alpha_{1,\text{HBI}}$	0.87 ± 0.23	0.89 ± 0.21
$\alpha_{2,\text{HBI}}$	0.86 ± 0.15	0.87 ± 0.14
$\alpha_{1,\text{SBP}}$	1.26 ± 0.20	1.27 ± 0.18
$\alpha_{2,\text{SBP}}$	0.83 ± 0.14	0.85 ± 0.13
$\alpha_{1,\text{DBP}}$	1.19 ± 0.17	1.19 ± 0.16
$\alpha_{2,\text{DBP}}$	0.75 ± 0.15	0.77 ± 0.15
α_{RES}	0.68 ± 0.07	0.73 ± 0.15

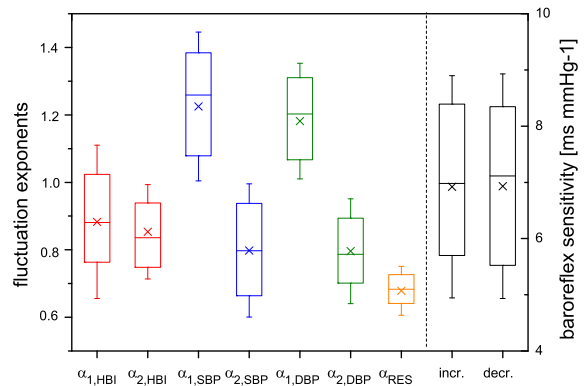


Fig. 3. Comparison of averages, medians, and standard deviations of the fluctuation exponents for HBI, SBP, DBP, RES, and BRS.

The results of CMA are additionally depicted together with the 25% and 75% quartiles and standard deviations in Fig. 3. Clearly, both blood pressure time series are non-stationary on short time scales ($\alpha_1 > 1$), where HBIs are stationary ($\alpha_1 < 1$). On long time scales, HBI, SBP and DBP show very similar stationary scaling behavior. Long-term respiratory correlations are still slightly weaker, see also [7].

The significances of the differences between the full sets of exponents for all 127 subjects are reported in the lower triangle of Table II. We see that most differences are significant except for those between $\alpha_{1,\text{HBI}}$ and $\alpha_{2,\text{HBI}}$, $\alpha_{1,\text{SBP}}$ and $\alpha_{1,\text{DBP}}$, as well as $\alpha_{i,\text{HBI}}$ and $\alpha_{2,\text{SBP}}$ ($i = 1, 2$). These results clearly show (i) the absence of a systematic crossover in HBI time series and (ii) the equivalence of SBP and DBP time series regarding their scaling behavior. Surprisingly, the small decrease of $\alpha_{2,\text{DBP}}$ compared with $\alpha_{2,\text{HBI}}$ is significant, although the values are fairly close to each other (see Fig. 3). Nevertheless, the similarity of the long-term scaling exponents suggests that a recent analysis of blood pressure fluctuations in rats [19] is probably also valid for humans. In this study somewhat similar scaling behavior was observed for controls but blood pressure signals became non-stationary also on large time scales for rats with surgically denervated baroreceptors.

The upper triangle of Table II reports the results of a cross-correlation analysis, in which we calculated the correlation coefficients r for linear fits in graphs of one variable plotted versus another one. Large coefficients r indicate that, e. g., a large (small) value of $\alpha_{1,\text{SBP}}$ in several subjects coincides with a large (small) value of $\alpha_{1,\text{DBP}}$ in the same subjects ($r = 0.57$ in this case). Clearly, noticeable correlations (0.38 – 0.57) exist between all α_1 values, indicating related short-term scaling behavior. This is somewhat surprising, given the previous results of very different effective scaling exponent α_1 for HBI and blood pressure series. It shows that, despite the non-stationarity of the blood pressure values, the regulation mechanisms for both types of autonomic functions are not independent of each other on short time scales. We speculate that these relations are caused by the fast branch of the baroreflex mechanism, while the slow branch causes the similar long-term scaling exponents α_2 . The inter-subject variations of $\alpha_{2,\text{HBI}}$ and $\alpha_{2,\text{DBP}}$, as well as $\alpha_{2,\text{SBP}}$, are noticeably cross-

TABLE II

UPPER TRIANGLE: CROSS-CORRELATION COEFFICIENTS OF ALL SCALING EXPONENTS AND BRS INDICES. LARGE CROSS-CORRELATION COEFFICIENTS ARE MARKED IN BOLD PRINT. LOWER TRIANGLE: T TEST PROBABILITIES FOR EQUIVALENCE OF THE CORRESPONDING TWO VARIABLES.

	$\alpha_{1,HBI}$	$\alpha_{2,HBI}$	$\alpha_{1,SBP}$	$\alpha_{2,SBP}$	$\alpha_{1,DBP}$	$\alpha_{2,DBP}$	α_{RES}	BRS _{incr.}	BRS _{decr.}
$\alpha_{1,HBI}$		-0.03	0.38	0.01	0.48	-0.03	0.10	-0.14	-0.13
$\alpha_{2,HBI}$	n.s.		-0.05	0.25	-0.05	0.23	-0.10	0.10	0.10
$\alpha_{1,SBP}$	$p < 0.001$	$p < 0.001$		-0.14	0.57	-0.09	-0.16	-0.03	-0.02
$\alpha_{2,SBP}$	n.s.	n.s.	$p < 0.001$		-0.17	0.73	-0.09	-0.04	-0.03
$\alpha_{1,DBP}$	$p < 0.001$	$p < 0.001$	n.s.	$p < 0.001$		-0.20	-0.04	-0.06	-0.05
$\alpha_{2,DBP}$	$p < 0.001$		0.09	-0.03	-0.03				
α_{RES}	$p < 0.001$		0.26	0.27					
BRS _{incr.}	-	-	-	-	-	-	-		0.99
BRS _{decr.}	-	-	-	-	-	-	-	n.s.	

correlated (see Table II). However, most of the corresponding coefficients are not very large, and these results are, therefore, not very reliable. Cross-correlations for respiratory scaling exponents are too weak for specific conclusions in all cases.

The average BRS values, also shown in Fig. 3, are very similar for both, increasing and decreasing SBP sequences. The large quartile ranges and standard deviations are caused by quite large inter-subject differences. The extremely high cross-correlation coefficient 0.99 of both BRS values shows that there are variations between subjects only, and both BRS values are practically identical for each individual in our study. Surprisingly, BRS values are quite strongly cross-correlated with the scaling exponents of respiration (see Table II). This relation might be a possible hint towards the gating theory [20], which suggests a modulation of BRS by respiration phase. However, more investigations are needed in order to confirm such a relationship. For example, the relation between respiratory auto-correlations and BRS might also be due to the way we calculated BRS using the dual sequence method, because respiratory intervals cause a high frequency variation of heartbeat intervals and therefore might also be the reason for many dual sequences used in the BRS calculations.

IV. CONCLUSION

In conclusion, we have studied the scaling behavior of fluctuations in HBI, SBP, DBP, and RES signals by employing CMA and DFA1. The results show that both methods are equivalent. Since the subjects are young, heartbeat fluctuations exhibit a rather homogeneous scaling behavior with very similar effective scaling exponents on small and large time scales. The scaling behavior of both types of blood pressure fluctuations, however, is characterized by non-stationary behavior on short time scales and stationary behavior similar to heartbeat on large time scales. These findings support very recent similar observations in rats, which led to the conclusion that the slow baroreflex control loop is responsible for long-term blood pressure regulation on time scales above 35 heartbeats [19]. Long-term auto-correlations in respiration are somewhat weaker and hardly correlated with heartbeat or blood pressure auto-correlations. However, surprisingly, respiratory auto-correlations seem to be related with baroreflex sensitivity – a hint towards the gating theory [20] that suggests further exploration.

ACKNOWLEDGMENT

The authors would like to thank the European Union project SOCIONICAL for financial support.

REFERENCES

- [1] M. Kobayashi and T. Musha. *IEEE Trans. Biomed. Eng.* 1982;29:456–7.
- [2] J. P. Saul, P. Albrecht, R. D. Berger, and R. J. Cohen. *Comput. Cardiol.* 1988;14:419–22.
- [3] C. K. Peng, S. Havlin, H. E. Stanley, and A. L. Goldberger. *Chaos* 1995;5:82–7.
- [4] A. Bunde, S. Havlin, J.W. Kantelhardt, T. Penzel, J.H. Peter, and K. Voigt. *Phys. Rev. Lett.* 2000;85:3736–39.
- [5] P. Ch. Ivanov, L. A. N. Amaral, A. L. Goldberger, et al. *Chaos* 2001;11:641–52.
- [6] T. Penzel, J. W. Kantelhardt, L. Grote, J.-H. Peter, and A. Bunde. *IEEE Trans. Biomed. Eng.* 2003;50:1143–51.
- [7] A. Y. Schumann, R. P. Bartsch, T. Penzel, P. Ch. Ivanov, and J. W. Kantelhardt. *Sleep* (in press, 2010).
- [8] M. Baumert, V. Baier, and A. Voss. *Fluct. and Noise Lett.* 2005;5:L549–55.
- [9] P. Castiglioni, G. Parati, A. Civijian, L. Quintin, and M. Di Rienzo. *IEEE Biomed. Eng.* 2009;56:675–84.
- [10] C. K. Peng, J. E. Mietus, Y. H. Liu et al. *Ann. Biomed. Eng.* 2002;30:683–92.
- [11] S. Rostig, J. W. Kantelhardt, T. Penzel, et al. *Sleep* 2005;28:411–7.
- [12] U. Frey, T. Brodbeck, A. Majumdar, et al. *Nature* 2005;438:667–70.
- [13] K. Linkenkaer-Hansen, V. V. Nikouline, J. M. Palva, and R. J. Ilmoniemi. *J. Neurosci.* 2001;21:1370–7.
- [14] Y. Shen, E. Olbrich, P. Achermann, and P. F. Meier. *Clin. Neurophysiol.* 2003;114:199–209.
- [15] F. Gans, A. Y. Schumann, J. W. Kantelhardt, T. Penzel, and I. Fietze. *Phys. Rev. Lett.* 2009;102:098701.
- [16] J. M. Hausdorff, P. L. Purdon, C. K. Peng, Z. Ladin, J. Y. Wei, and A. L. Goldberger. *J. Appl. Physiol.* 1996;80:1448–57.
- [17] R. Bartsch, M. Plotnik, J. W. Kantelhardt, S. Havlin, N. Giladi, and J. M. Hausdorff. *Physica A* 2007;383:455–65.
- [18] A. Voss, R. Schroeder, S. Truebner, M. Goernig, H. R. Figulla, and A. Schirdewan. *Chaos* 2007;17:015120.
- [19] C. E. C. Galhardo, T. J. P. Penna, M. Argollo de Menezes, and P. P. S. Soares. *New J. Phys.* 2009;11:103005.
- [20] D. L. Eckberg. *J. Physiol.* 2003;548:339–52.
- [21] R. Schneider. Opensource toolbox, available at www.librasch.org.
- [22] J. Alvarez-Ramirez, E. Rodriguez, and J. C. Echeverria. *Physica A* 2005;354:199.
- [23] A. Bashan, R. P.Bartsch, J. W. Kantelhardt, and S. Havlin. *Physica A* 2008;387:5080–90
- [24] C. K. Peng, S. V. Buldyrev, S. Havlin, M. Simons, H. E. Stanley, and A. L. Goldberger. *Phys. Rev. E* 1994;49:1685–9.
- [25] J. W. Kantelhardt, E. Koscielny-Bunde, H. H. A. Rego, S. Havlin, and A. Bunde. *Physica A* 2001;295:441–54.
- [26] M. I. Bogachev, O. V. Mamontov, A. O. Konradi, Y. D. Uljanitski, J. W. Kantelhardt, and E. V. Schlyakhto. *Physiol. Meas.* 2009;30:631–45.